

**Cite this article as:** Luo Hengjun, Deng Hao, Yuan Wuhua, et al. Effect of Heat Treatment Holding Time on Microstructure and Tensile Properties of Ti55511 Alloy[J]. Rare Metal Materials and Engineering, 2025, 54(05): 1185-1193. DOI: <https://doi.org/10.12442/j.issn.1002-185X.20240192>.

ARTICLE

# Effect of Heat Treatment Holding Time on Microstructure and Tensile Properties of Ti55511 Alloy

Luo Hengjun<sup>1,2</sup>, Deng Hao<sup>2</sup>, Yuan Wuhua<sup>1</sup>, Liu Wenhao<sup>3</sup>, Chen Longqing<sup>4</sup>

<sup>1</sup> College of Materials Science and Engineering, Hunan University, Changsha 410082, China; <sup>2</sup> China National Erzhong Group Deyang Wanhang Die Forging Co., Ltd, Deyang 618000, China; <sup>3</sup> College of Physics, Sichuan University, Chengdu 610065, China; <sup>4</sup> Key Laboratory of Radiation Physics and Technology, Ministry of Education, Institute of Nuclear Science and Technology, Sichuan University, Chengdu 610065, China

**Abstract:** The effect of holding time of double annealing process on the microstructure and mechanical properties of Ti-5Al-5Mo-5V-1Cr-1Fe (Ti55511) alloy was investigated. Results reveal that the shape and size of the primary  $\alpha$  ( $\alpha_p$ ) phase are predominantly influenced by the holding time at the first stage. With the prolongation of holding time, the long strip of  $\alpha_p$  is transformed into a short rod due to the terminal migration mechanism, leading to the broadening growth, and the growth of  $\alpha_p$  slows down when the holding time is over 2 h. The volume fraction of  $\alpha_p$  is mainly affected by the holding time of the second stage: with the prolongation of holding time, the volume fraction of  $\alpha_p$  is increased, which is accompanied by the precipitation of the secondary  $\alpha$  ( $\alpha_s$ ). The mechanical properties of Ti55511 alloy are influenced by both  $\alpha_p$  and  $\alpha_s$ . Tensile results indicate that the optimal holding time of double annealing is 1–4 h for the first stage and 0.5–2 h for the second stage.

**Key words:** Ti55511 alloy; heat treatment; holding time; microstructure; tensile property

## 1 Introduction

Over the past few decades, titanium alloys have evolved into a crucial structural material in aerospace, which is attributed to their commendable mechanical properties and corrosion resistance<sup>[1–5]</sup>. Ongoing research efforts have further enhanced the comprehensive mechanical properties of titanium alloys. A series of innovative microstructure and composition designs for titanium alloy have emerged, significantly contributing to the advancement of the aerospace field<sup>[6–9]</sup>.

Currently, foundational theories regarding titanium alloys have been firmly established. The phases of titanium alloys primarily consist of two isomers: the body-centered cubic  $\beta$  phase prevailing at elevated temperatures and the hexagonal close-packed  $\alpha$  phase reigning at lower thermal thresholds<sup>[8]</sup>. The equilibrium between these states may be deftly adjusted through meticulous manipulation of the ratio of  $\alpha$ -stable element to  $\beta$ -stable element<sup>[10]</sup>. Conventionally, the hexagonal  $\alpha$  phase, which is characterized by a less extensive slip system,

augments structural integrity and exhibits reduced susceptibility to deformation. Conversely, the body-centered cubic  $\beta$  phase, boasting a plethora of slip systems, chiefly confers plasticity upon the alloy matrix<sup>[11]</sup>. For the  $\alpha+\beta$  titanium alloys with specific composition, their mechanical properties predominantly hinge on the size, morphology, and volume fraction of the  $\alpha$  phase, which can be fine-tuned through thermal deformation and heat treatment<sup>[12–15]</sup>.

Ti-5Al-5Mo-5V-1Cr-1Fe (Ti55511) alloy derived from the BT22 alloy is a  $\beta$  titanium alloy with high strength and high toughness, which usually serves as a versatile substitute for high-strength steel and Ti-6Al-4V alloy in aircraft structural materials, significantly reducing mass by 15%–20%. Notably, Ti55511 alloy excels in weldability, showing extensive application potential in crucial aircraft components, such as main landing gear, wing spar, and beam parts<sup>[15–17]</sup>.

As a typical near- $\beta$  titanium alloy, Ti55511 exhibits a microstructure comprising  $\alpha$  and  $\beta$  phases, and its mechanical properties are highly dependent on these phases.

Received date: April 02, 2024

Corresponding author: Yuan Wuhua, Ph. D., Professor, College of Materials Science and Engineering, Hunan University, Changsha 410082, P. R. China, E-mail: yuan46302@163.com

Copyright © 2025, Northwest Institute for Nonferrous Metal Research. Published by Science Press. All rights reserved.

Consequently, extensive investigations have studied the influence of thermomechanical processing and heat treatment on the microstructure of Ti55511 alloy, elucidating its correlation with mechanical properties<sup>[18-19]</sup>. For instance, Liu et al<sup>[20]</sup> introduced a multi-heat treatment regimen for Ti55511 alloy. The multi-step aging method promotes uniform precipitation behavior of secondary  $\alpha$  ( $\alpha_s$ ) phase, resulting in a bimodal microstructure with commendable mechanical properties. Wu et al<sup>[21]</sup> devised an optimized heat treatment for alloys with Widmannstätten microstructure, focusing on high cycle fatigue behavior. Ran et al<sup>[22]</sup> explored various heat treatments to produce Ti55511 alloy samples with diverse structures and analyzed their tensile behavior under different strain rates and temperatures. It is revealed that the basket-weave microstructure exhibits superior strength but lower elongation, whereas the Widmannstätten microstructure displays the opposite characteristics. Despite these findings, research also suggests that the basket-weave microstructure excels in high-temperature creep resistance, durability, fracture toughness, and fatigue crack propagation resistance, which should be further investigated<sup>[23]</sup>. Yin et al<sup>[24]</sup> revealed that diverse deformation during forging exerts negligible influence on the basket-weave microstructure developed through subsequent heat treatment. Nonetheless, variations in the mechanical properties of the alloys can be observed under distinct deformation conditions. Shi et al<sup>[23]</sup> highlighted the direct impact of solution temperatures of double heat treatment on the morphology and size of  $\alpha_p$  in the basket-weave microstructure after quasi- $\beta$  forging, proposing a predictive model for the alloy microstructure.

The tensile properties of Ti55511 alloy after quasi- $\beta$  forging are notably influenced by pivotal parameters, including forging deformation, heat treatment temperature, and holding time. These critical factors intricately impact the morphology, dimensions, and content of primary  $\alpha$  ( $\alpha_p$ ) phase within the microstructure, which result from diverse deformation mechanisms and strengthening effects of the  $\alpha$  phase during tensile loading, thereby yielding significant disparities in strength and ductility<sup>[25-26]</sup>. Wang et al<sup>[27]</sup> investigated the precipitation dynamics of the  $\alpha$  phase in the Ti55511 alloy under high-temperature compression. It was found that the distribution of the  $\alpha$  phase remains unaffected by deformation parameters. However, as the deformation temperature rises, the content, aspect ratio, and size of the  $\alpha$  phase decrease. Conversely, an increase in strain rate leads to a rise in content, aspect ratio, and size of the  $\alpha$  phase at first and then a decrease. Lin et al<sup>[28]</sup> investigated the impact of solution temperature on both the  $\alpha$  phase and mechanical properties of the forged Ti55511 alloy. The findings revealed that as the temperature rises, the content and size of  $\alpha_p$  decrease, whereas those of  $\alpha_s$  increase. Moreover, with the increase in temperature, the ultimate tensile strength (UTS) and yield strength (YS) of the alloy initially increase and then decrease, and the elongation decreases. Currently, the influence of heat treatment holding time on the microstructure and tensile properties of Ti55511 titanium alloy is rarely reported.

Establishing a comprehensive relationship among heat treatment parameters, microstructure morphology, and tensile properties is imperative. Such an understanding holds immense significance in guiding the optimization of the heat treatment. In this research, two heat preservation processes, which have great influence on the microstructure during double annealing, were studied. After identifying the optimal annealing temperature, the influence of the holding time of double annealing on the morphology, size, and content of  $\alpha_p$  as well as the precipitation of  $\alpha_s$  was investigated. The evolution of the microstructure under different heat treatment parameters was analyzed, leading to the formulation of a comprehensive relationship among heat treatment parameters, microstructure, and mechanical properties.

## 2 Experiment

The raw material for Ti55511 alloy was cut from a bar of 300 mm in length (supplied by Western Superconducting Technologies Co., Ltd) with the measured  $\beta$  phase transition temperature ( $T_\beta$ ) of 870 °C. The bar was subjected to a quasi- $\beta$  forging and formed a typical basket-weave microstructure. To investigate the influence of holding time on the microstructure and tensile properties of Ti55511 alloy, the bar was subjected to a quasi- $\beta$  forging. Square samples with the dimension of 30 mm×30 mm×100 mm were cut from forged Ti55511 bar for double annealing treatment. The impact of the first stage (T1, 830–840 °C) and the second stage (T2, 740–750 °C) of holding process during the double annealing process of Ti55511 alloy on the microstructure and mechanical properties was studied. The heat treatment process (double annealing) is illustrated in Fig. 1 (air cooling is denoted as AC), and the conditions for the orthogonal experiment are listed in Table 1 (furnace cooling is denoted as FC).

The annealed samples underwent grinding with SiC sandpaper (220#–2000#), followed by polishing using silica suspension (0.06  $\mu$ m) on a polishing machine. Subsequently, the sample surface was subjected to corrosion using Kroll reagent (4 mL HF+6 mL HNO<sub>3</sub>+90 mL H<sub>2</sub>O). The resultant microstructure was observed by Leica DMi8C optical microscope (OM), JSM-IT500HR scanning electron micro-

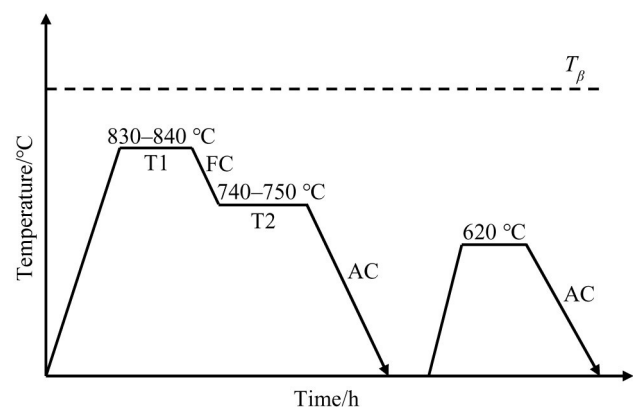


Fig.1 Schematic diagram of heat treatment process for Ti55511 alloy

**Table 1** Different heat treatments for Ti55511 samples

| Sample        | Heat treatment                                     | Holding time/h            |
|---------------|--|---------------------------|
| HT1- <i>X</i> | 830 °C/ <i>X</i> h FC to 750 °C/2 h AC, 620 °C/4 h | <i>X</i> =0.5, 1, 2, 3, 4 |
| HT2- <i>X</i> | 840 °C/ <i>X</i> h FC to 750 °C/2 h AC, 620 °C/4 h | <i>X</i> =0.5, 1, 2, 3, 4 |
| HT3- <i>X</i> | 840 °C/2 h FC to 740 °C/ <i>X</i> h AC, 620 °C/4 h | <i>X</i> =0.5, 1, 2, 3, 4 |
| HT4- <i>X</i> | 840 °C/2 h FC to 750 °C/ <i>X</i> h AC, 620 °C/4 h | <i>X</i> =0.5, 1, 2, 3, 4 |

scope (SEM), and FEI Titan G2 60-300 transmission electron microscope (TEM). The average thickness (width) of the  $\alpha_p$  was determined using the intercept method, and no less than 200  $\alpha_p$  were measured for each sample. Measurements were conducted three times to obtain an average value and variance calculation for analysis. The  $\alpha_p$  content was assessed via Image Pro software using the area method. This experiment was conducted three times to obtain an average value and variance calculation for analysis.

The samples subjected to different annealing conditions were precisely cut into the specified dimension by electric spark cutter for tensile tests, as shown in Fig.2. Tensile testing at room temperature was conducted on an Instron 8801 universal mechanical test machine, following the procedures in GB/T 228.1-2021 standard. The testing rate was set as 0.5 mm/min, and each experiment was replicated no less than three times. The average value of the experimental results was computed, and the variance was also calculated.

### 3 Results and Discussion

#### 3.1 Effect of holding time of T1 stage on microstructure

HT2 series samples were selected as typical ones to investigate the influence of holding time of T1 stage on microstructures, and their microstructures are shown in Fig.3. When the temperature is maintained at 840 °C for 0.5 h, the  $\alpha_p$  phase in the sample exhibits a slender morphology. With the prolongation of holding time at T1 stage, the  $\alpha_p$  phase is gradually coarsened and transformed from slender to short rod-like structures, indicating a reduction in the aspect ratio of the  $\alpha_p$  phase. Statistical analysis of the thickness and content of the  $\alpha_p$  phase is shown in Fig.4. It can be seen that when the holding temperature is 830 and 840 °C and the holding time is less than 2 h, the thickness of the  $\alpha_p$  phase significantly increases with the prolongation of holding time. When the holding time is more than 2 h, the thickness of the  $\alpha_p$  phase exhibits a slower growth trend, as illustrated in Fig. 4a.

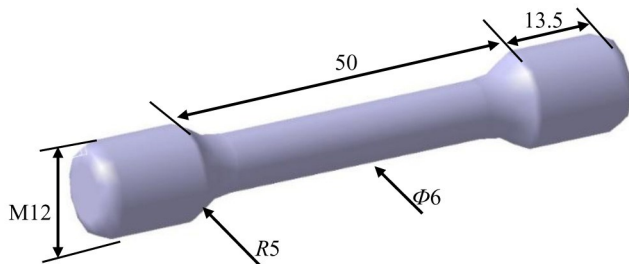


Fig.2 Schematic diagram of tensile sample

Therefore, a relationship describing the influence of holding time on the thickness of the  $\alpha_p$  phase ( $T_{\alpha_p}$ ) can be expressed by Eq.(1), as follows:

$$T_{\alpha_p} = 1.82 - 1.29 \exp\left(-\frac{t}{0.83}\right) \quad (1)$$

where  $T_{\alpha_p}$  represents the thickness of the  $\alpha_p$  phase ( $\mu\text{m}$ ), and  $t$  denotes the holding time (h).

Fig.4b presents the content of the  $\alpha_p$  phase ( $V_{\alpha_p}$ ) in different samples. The results indicate that when the holding temperature is 830 and 840 °C, the content of  $\alpha_p$  phase exhibits discernible evolutionary trend with the prolongation of holding time. The content of  $\alpha_p$  phase consistently falls within the range of 32.9vol%–33.9vol%, suggesting that the holding time exerts minimal influence on the content of the  $\alpha_p$  phase.

The Ti55511 alloy undergoes the  $\beta \rightarrow \alpha_p$  reaction during the T1 stage, wherein the  $\alpha_p$  phase is precipitated owing to element diffusion amidst lattice distortion induced by forging deformation. Subsequently, during the holding stage, the precipitated  $\alpha_p$  phase continues to grow through element diffusion at the grain boundary. Therefore, under substantial lattice distortion (serving as the phase transition driving force) with a sufficient activation energy source (achieved through high temperature), the holding time becomes crucial in the determination of the extent of element diffusion<sup>[27]</sup>. In essence, the longer the holding time, the more comprehensive the diffusion growth of the  $\alpha_p$  phase. To corroborate this hypothesis, Ti55511 alloy forged in quasi- $\beta$  form was held at 840 °C for 0.5 and 2 h followed by rapid water quenching (WQ), and the resultant microstructures are depicted in Fig.5a and 5b, respectively. It can be seen that the  $\alpha_p$  phase is fully precipitated and becomes larger when the holding time is 2 h during the T1 stage. With the prolongation of holding time in the T1 stage, the  $\beta \rightarrow \alpha_p$  reaction becomes more pronounced, resulting in an augmentation of the thickness of the  $\alpha_p$  phase. However, with the prolongation of holding time, the element diffusion between the  $\alpha_p$  phase and the  $\beta$  matrix tends to attain a dynamic equilibrium, decelerating the growth of both phases.

Moreover, the elongated  $\alpha_p$  phase predominantly undergoes growth propelled by the terminal migration mechanism. This mechanism involves the migration of grain boundaries under the influence of interfacial tension. Grain boundary migration  $M$  can be quantified by Eq.(2), as follows:

$$M = M_0 e^{-\frac{Q}{kT}} \quad (2)$$

where  $M_0$  denotes the initial grain boundary mobility;  $K$  signifies curvature;  $T$  signifies temperature;  $Q$  and  $e$  are constants. Notably, Eq. (2) elucidates that grain boundary

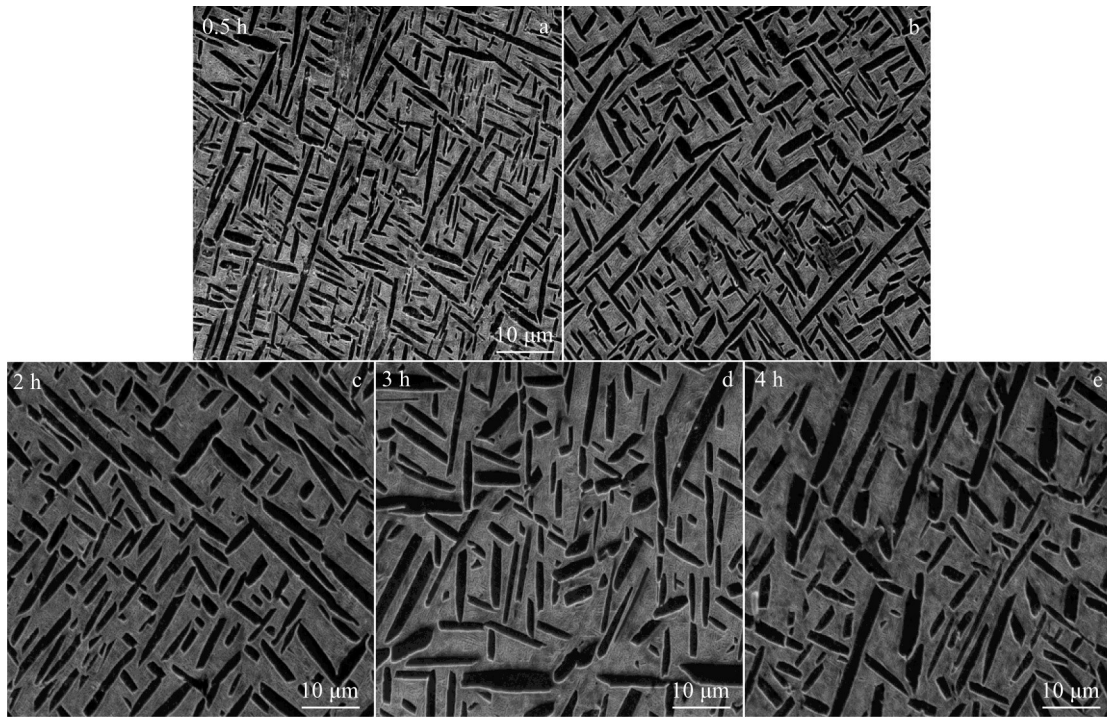


Fig.3 SEM microstructures of HT2- $X$  samples: (a)  $X=0.5$ , (b)  $X=1$ , (c)  $X=2$ , (d)  $X=3$ , and (e)  $X=4$

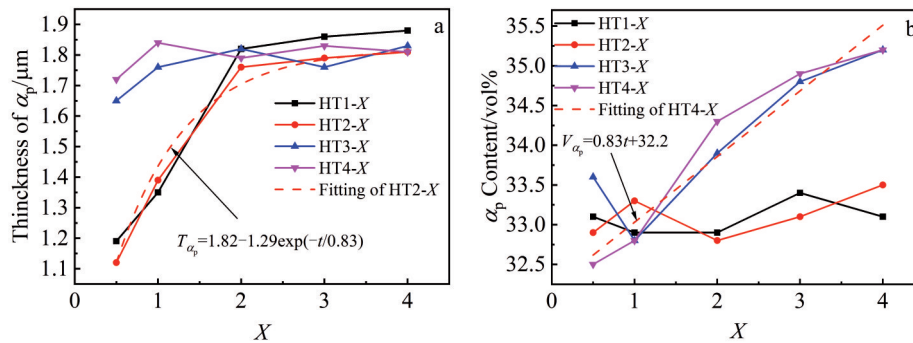


Fig.4 Thickness (a) and content (b) of  $\alpha_p$  in HT1- $X$ , HT2- $X$ , HT3- $X$ , and HT4- $X$  samples

mobility is inversely proportional to the curvature radius.

As shown in Fig.5c–5e, the curvature radius  $r_1$  at the end is smaller than the curvature radius  $r_2$  on both sides, and a smaller curvature radius engenders a greater interface driving force during diffusion. Consequently, for heat preservation, with the prolongation of time, elements migrate from the end area of the  $\alpha_p$  phase to both sides, leading to the transformation of the  $\alpha_p$  phase from slender to short-rod structures during the long heat preservation period<sup>[29–30]</sup>.

The holding time during the T1 stage has minimal impact on the content of the  $\alpha_p$  phase, and subsequent T2 stage leads to the continuous decomposition of the residual  $\beta$  phase and the continuous precipitation of the  $\alpha_p$  phase. Due to identical conditions in subsequent stages, the driving force for the transformation of the residual  $\beta$  phase into the  $\alpha_p$  phase remains consistent, resulting in little change in its content<sup>[31]</sup>. Hence, the holding time of T1 stage significantly influences the thickness and morphology of the  $\alpha_p$  phase but has a little

impact on its content during the double annealing process of Ti55511 alloy.

### 3.2 Effect of holding time of T2 stage on microstructure

The impact of holding time of T2 stage on the microstructure of Ti55511 alloy was analyzed through the results of HT3 series samples. SEM microstructures of HT3- $X$  samples are shown in Fig. 6. The thickness of the  $\alpha_p$  phase exhibits a slight increase when the holding time of T2 stage is prolonged from 0.5 h to 1 h. For instance, the width of the  $\alpha_p$  phase is 1.65  $\mu\text{m}$  when the holding time of T2 stage is 0.5 h and 1.76  $\mu\text{m}$  when the holding time of T2 stage is 1 h. However, when the holding time of T2 stage is over 1 h, the thickness of the  $\alpha_p$  phase does not show a clear growth trend. The holding time of T2 stage significantly influences the content of the  $\alpha_p$  phase. According to Fig.4b, the content of the  $\alpha_p$  phase exhibits an increasing trend with the prolongation of holding time. The content of the  $\alpha_p$  phase in HT3-0.5, HT3-1, HT3-2, HT3-3, and HT3-4 samples is 33.6vol%, 32.8vol%,

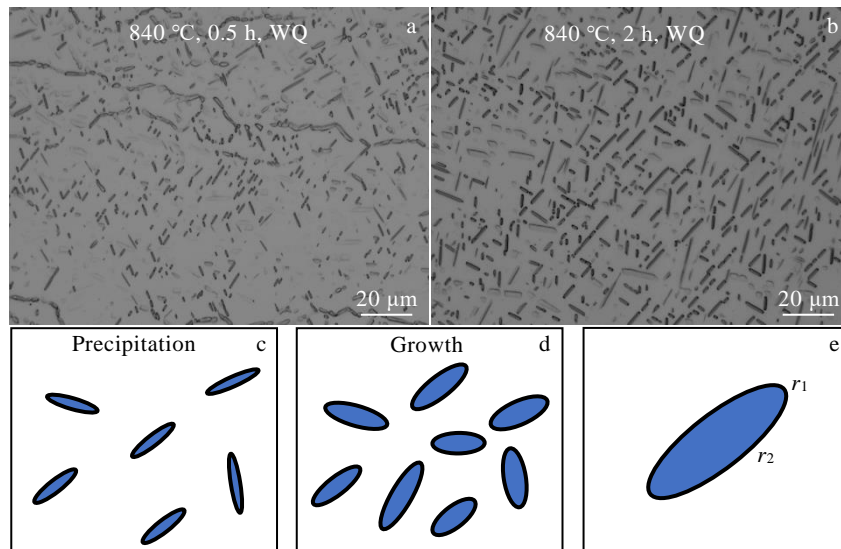


Fig.5 OM microstructures of Ti55511 samples heat treated at 840 °C/0.5 h WQ (a) and 840 °C/2h WQ (b) during T1 stage; schematic diagrams of precipitation and growth process of  $\alpha_p$  (c–e)

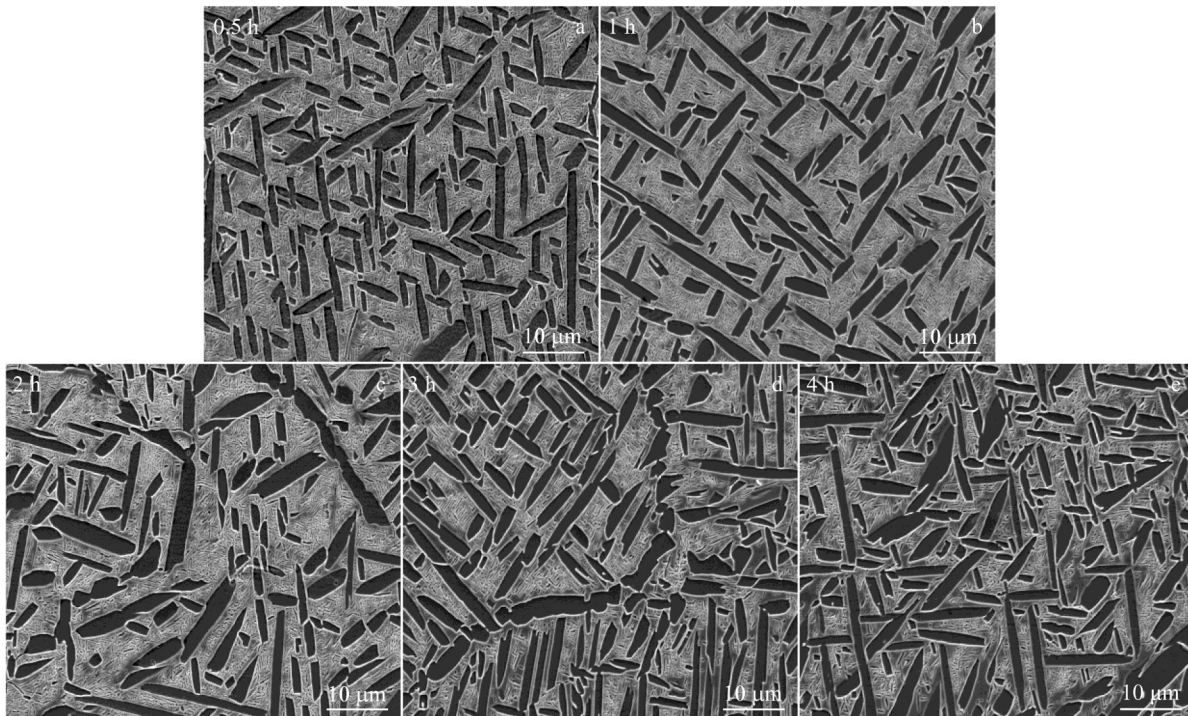


Fig.6 SEM microstructures of HT3- $X$  samples: (a)  $X=0.5$ , (b)  $X=1$ , (c)  $X=2$ , (d)  $X=3$ , and (e)  $X=4$

33.9vol%, 34.8vol%, and 35.2vol%, respectively. The content of the  $\alpha_p$  phase in HT4-0.5, HT4-1, HT4-2, HT4-3, and HT4-4 samples is 32.5vol%, 32.8vol%, 34.3vol%, 34.9vol%, and 35.3vol%, respectively. Therefore, the relationship between the content of the  $\alpha_p$  phase ( $V_{\alpha_p}$ ) and holding time of T2 stage ( $t$ ) can be expressed by Eq.(3), as follows:

$$V_{\alpha_p} = 0.83t + 32.2 \quad (3)$$

In general, titanium alloy undergoes the  $\beta \rightarrow \alpha$  transformation once the temperature is within the temperature range of the two-phase region. Consequently, titanium alloy

forged at the temperature of  $\beta$ -phase region completes  $\alpha$  phase precipitation and initial growth during T1 stage. Once the subsequent temperature reduces, the residual  $\beta$  phase undergoes further decomposition, and additional  $\alpha$  phase is precipitated. In the subsequent T2 stage, the continuous precipitation and growth of  $\alpha_p$  can be delineated into three stages. (1) With the decrease in temperature and the prolongation of heat preservation, the kinetic conditions for  $\alpha_p$  precipitation become increasingly favorable, and the  $\beta \rightarrow \alpha_p$  reaction involving element diffusion persists from the T1 stage. (2) Adjacent  $\alpha_p$  phases with the same orientation are in

contact and the grain boundary phase results in  $\alpha_p/\alpha_p$  phase growth during the diffusion process. (3) The growth of the  $\alpha_p$  phase stabilizes when  $\beta/\alpha_p$  element diffusion tends to dynamic equilibrium, leading to the high enrichment of  $\beta$  stable elements in the  $\beta$  matrix<sup>[32]</sup>. To identify the evidence of  $\alpha_p$  phase growth in the aforementioned second stage, samples were subjected to WQ after heat treatment at 840 °C/2 h FC to 740 °C/0 h and 840 °C/2 h FC to 740 °C/2 h. OM microstructures are shown in Fig. 7. The coalescent growth of the  $\alpha_p/\alpha_p$  phase is already initiated during FC stage, becoming more apparent in the subsequent heat preservation process, as indicated by the arrows in Fig.7. Apparently, the content of the  $\alpha_p$  phase increases with the prolongation of the holding time of T2 stage.

### 3.3 Tensile property

Fig. 8 shows the tensile properties of HT1-*X* and HT2-*X* samples. In addition, the representative engineering stress-engineering strain curves are shown in Fig. 9. The results suggest that with the prolongation of holding time, there is no clear trend in UTS and YS of the samples with the strength difference being less than 10 MPa. However, a noticeable increase in the elongation can be observed when the holding time is prolonged to 1 h. The elongation of HT1-0.5, HT1-1, HT1-2, HT1-3, and HT1-4 samples is 12.5%, 14.8%, 15.1%, 14.9%, and 14.8%, respectively. Similarly, the elongation of HT2-0.5, HT2-1, HT2-2, HT2-3, and HT2-4 samples is 12.1%, 14.1%, 14.3%, 14.9%, and 14.7%, respectively. The strength of titanium alloys is primarily governed by the  $\alpha_s$

phase after aging treatment, and there is a little variance in the kinetics of  $\alpha_s$  precipitation among samples when the  $\alpha_p$  contents are basically the same and the aging temperature is fixed. Consequently, the consistent precipitation behavior of  $\alpha_s$  leads to negligible changes in the strength of samples holding for different time. The larger elongation is attributed to the increased thickness of the  $\alpha_p$  phase, as the relatively larger  $\alpha_p$  phase expands the dislocation slip space, ensuring a concurrent increase in elongation<sup>[33]</sup>.

Fig. 10 shows the tensile properties of HT3-*X* and HT4-*X* samples. UTS and YS of the samples exhibit an initial increase, followed by a subsequent decrease with the prolongation of holding time, reaching their peak values when the holding time is 2 h. For HT3 series samples, UTS initially rises from 1101 MPa to 1122 MPa and then declines to 1096 MPa, whereas YS increases from 1015 MPa to 1031 MPa and finally decreases to 1010 MPa. Conversely, for HT4 series samples, UTS increases from 1104 MPa to 1118 MPa and then decreases to 1090 MPa; YS rises from 1011 MPa to 1023 MPa and finally declines to 1004 MPa. However, with the prolongation of holding time, the change in elongation of HT3 series samples exhibit an opposite trend to the change in strength, whereas the change in elongation of HT4 series samples show no clear trend. Fig.4 reveals that the content of the  $\alpha_p$  phase in the sample rises with the prolongation of holding time of T2 stage. As the content of the  $\alpha_p$  phase increases, there is a reduction in residual  $\beta$ -phase instances, leading to a high enrichment of  $\beta$ -stable elements in the

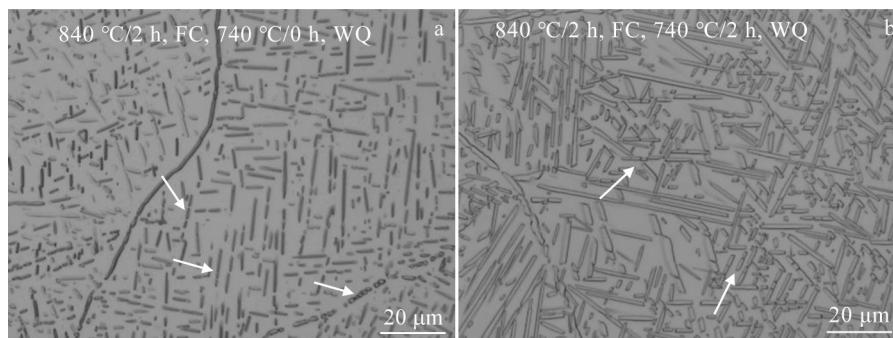


Fig.7 OM microstructures of Ti55511 samples heat treated at 840 °C/2 h FC to 740 °C/0 h WQ (a) and 840 °C/2 h FC to 740 °C/2 h WQ (b)

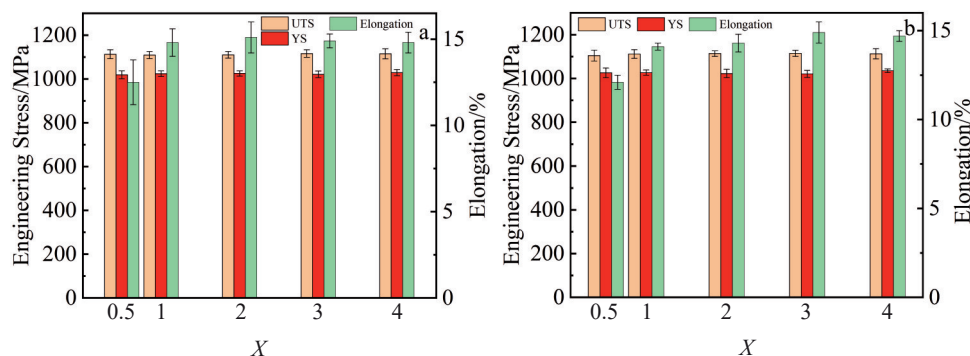


Fig.8 Tensile properties of Ti55511 samples heat treated at 830 °C/*X* h FC to 750 °C/2 h AC, 620 °C/4 h (a) and 840 °C/*X* h FC to 750 °C/2 h AC, 620 °C/4 h (b)

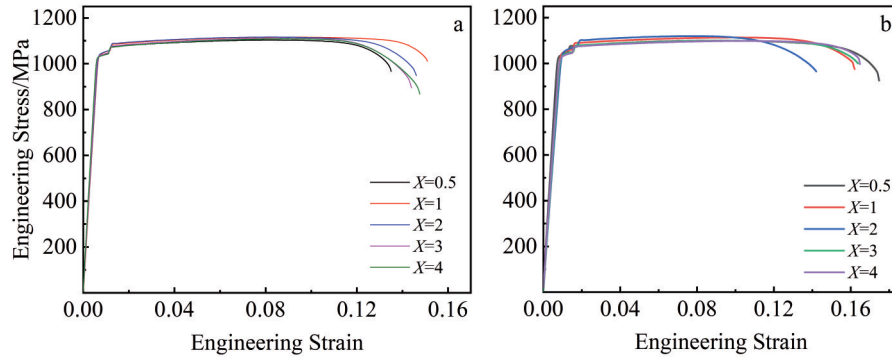


Fig.9 Engineering stress-engineering strain curves of Ti55511 samples heat treated at 840 °C/ $X$  h FC to 750 °C/2 h AC, 620 °C/4 h (a) and 840 °C/2 h FC to 750 °C/ $X$  h AC, 620 °C/4 h (b)

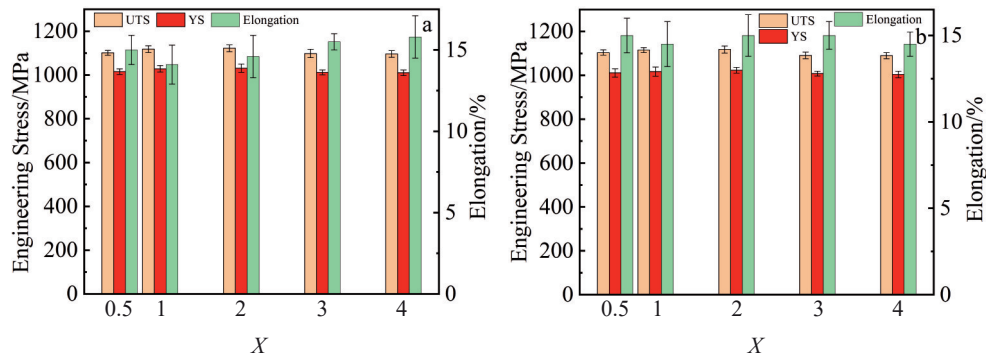


Fig.10 Tensile properties of HT3- $X$  and HT4- $X$  samples

$\beta$ -matrix. Consequently, this phenomenon diminishes the precipitation kinetics and available space for the  $\alpha_s$  phase, promoting a decline in the content of  $\alpha_s$  phase and henceforth a reduction in the sample strength<sup>[34]</sup>. To prove this conclusion, SEM and TEM were used to observe HT3-2 and HT3-4

samples, as shown in Fig. 11. It can be seen that when the content of  $\alpha_p$  phase is relatively small, the content of  $\alpha_s$  phase resolved by residual  $\beta$  phase is significantly larger, compared with the state when the content of  $\alpha_p$  phase is relatively large. Therefore, variation in contents of  $\alpha_p$  and  $\alpha_s$  definitely affect

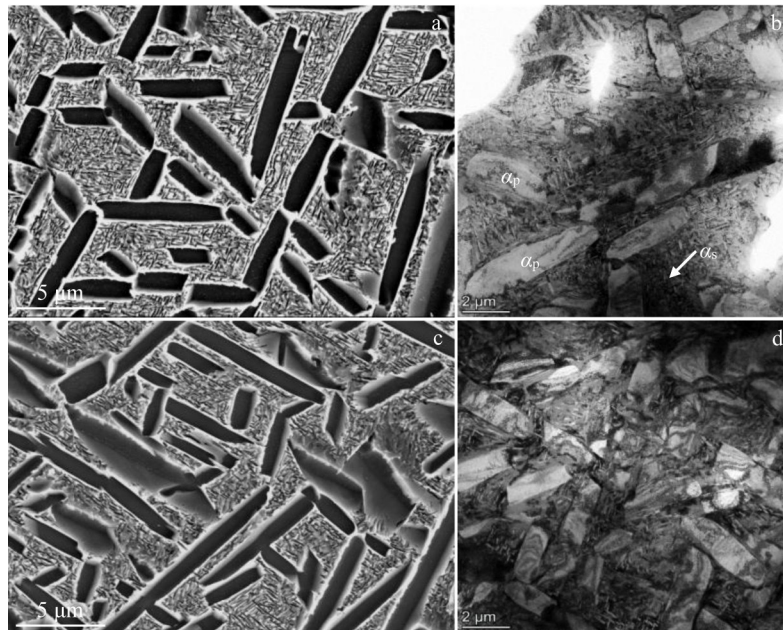


Fig.11 SEM (a, c) and TEM (b, d) images of HT3-2 (a-b) and HT3-4 (c-d) samples

the tensile strength of Ti55511 alloy.

Based on the abovementioned microstructure and mechanical properties, the optimal holding time range for Ti55511 titanium alloy can be determined: the effective holding time for the T1 stage is within the range of 1–4 h, and the effective holding time is 0.5–2 h for the T2 stage.

#### 4 Conclusions

1) The duration of the T1 stage in double annealing affects the shape and size of  $\alpha_p$ , but has minimal effect on its volume fraction. Conversely, the holding time of the T2 stage in double annealing impacts the volume fraction of  $\alpha_p$ , thereby influencing the precipitation of  $\alpha_s$ .

2) During the double annealing process,  $\alpha_p$  undergoes a transformation from long strip to short rod structure driven by the terminal migration mechanism, leading to broadening growth.

3) UTS and YS of Ti55511 alloy are influenced by the size and proportion of  $\alpha_p$  and  $\alpha_s$ . An increase in the size and volume fraction of  $\alpha_p$  corresponds to enhanced plasticity in the alloy, whereas the strength of the alloy is determined by  $\alpha_s$ .

4) Optimal holding time in the double annealing process for Ti55511 titanium alloy can be determined: the effective holding time for the T1 stage is within the range of 1–4 h, and the effective holding time is 0.5–2 h for the T2 stage.

#### References

- Banerjee D, Williams J C. *Acta Materialia*[J], 2013, 61(3): 844
- Li Silan, Li Qian, Zhang Siyuan et al. *Titanium Industry Progress*[J], 2024, 41(6): 7 (in Chinese)
- Li Yinghao, He Fei, Hou Fengqi et al. *Titanium Industry Progress*[J], 2014, 31(4): 20 (in Chinese)
- Wang Liya, Zheng Youping, Yang Liu et al. *Titanium Industry Progress*[J], 2022, 39(3): 22 (in Chinese)
- Yumak N, Aslantaş K. *Journal of Materials Research and Technology*[J], 2020, 9(6): 15360
- Rahulan N, Sharma S S, Rakesh N et al. *Materials Today: Proceedings*[J], 2022, 56: A7
- Li G, Chandra S, Rashid R A et al. *Journal of Manufacturing Processes*[J], 2022, 75: 72
- Gao P F, Fu M W, Zhan M et al. *Journal of Materials Science & Technology*[J], 2020, 39: 56
- Singh G, Ramamurty U. *Progress in Materials Science*[J], 2020, 111: 100653
- Yang L, Pang Z C, Ming L et al. *Materials Science and Engineering A*[J], 2019, 745: 440
- Hua K, Zhang Y L, Tong Y L et al. *Materials Science and Engineering A*[J], 2022, 840: 142997
- Zhang T, Liu C T. *Advanced Powder Materials*[J], 2022, 1(1): 100014
- Pushp P, Dasharath S M, Arati C. *Materials Today: Proceedings*[J], 2022, 54: 537
- He Longnong, An Xinglong, Wang Tao et al. *Titanium Industry Progress*[J], 2025, 42(1): 14 (in Chinese)
- Boyer R R. *Materials Science and Engineering A*[J], 1996, 213(1–2): 103
- Singh P, Pungotra H, Kalsi N S. *Materials Today: Proceedings*[J], 2017, 4(8): 8971
- Warchomicka F, Poletti C, Stockinger M. *Materials Science and Engineering A*[J], 2011, 528(28): 8277
- Cotton J D, Briggs R D, Boyer R R et al. *JOM*[J], 2015, 67(6): 1281
- Dong R F, Li J S, Kou H C et al. *Journal of Materials Science & Technology*[J], 2019, 35(1): 48
- Liu Z D, Du Z X, Jiang H Y et al. *Progress in Natural Science: Materials International*[J], 2021, 31(5): 731
- Wu G Q, Shi C L, Sha W et al. *Materials Science and Engineering A*[J], 2013, 575: 111
- Ran C, Sheng Z M, Chen P W et al. *Materials Science and Engineering A*[J], 2020, 773: 138728
- Shi X H, Zeng W D, Shi C L et al. *Journal of Alloys and Compounds*[J], 2015, 632: 748
- Yin M, Luo H J, Deng H et al. *Materials Science and Engineering A*[J], 2022, 853: 143786
- Li Y H Z, Ou X Q, Ni S et al. *Materials Science and Engineering A*[J], 2019, 742: 390
- Liu Z, Du Z, Jiang H et al. *Journal of Materials Research and Technology*[J], 2022, 17: 2528
- Wang Q W, Lin Y C, Jiang Y Q et al. *Materials Characterization*[J], 2019, 151: 358
- Lin Y C, Wang L H, Wu Q et al. *Materials Research Express*[J], 2019, 6(11): 1165
- Nag S, Banerjee R, Srinivasan R et al. *Acta Materialia*[J], 2009, 57(7): 2136
- Shekhar S, Sarkar R, Kar S K et al. *Materials & Design*[J], 2015, 66: 596
- Fan J K, Li J S, Kou H C et al. *Materials Characterization*[J], 2014, 96: 93
- Qin D Y, Lu Y F, Guo D Z et al. *Materials Science and Engineering A*[J], 2013, 587: 100
- Dehghan-Manshadi A, Dippenaar R J. *Materials Science and Engineering A*[J], 2011, 528(3): 1833
- Zhang X D, Evans D J, Baeslack Iii W A et al. *Materials Science and Engineering A*[J], 2003, 344(1–2): 300

## 热处理保温时间对 Ti55511 钛合金显微组织和拉伸性能的影响

罗恒军<sup>1,2</sup>, 邓浩<sup>2</sup>, 袁武华<sup>1</sup>, 刘文豪<sup>3</sup>, 陈龙庆<sup>4</sup>

(1. 湖南大学 材料科学与工程学院, 湖南 长沙 410082)

(2. 中国第二重型机械集团德阳万航模锻有限责任公司, 四川 德阳 618000)

(3. 四川大学 物理学院, 四川 成都 610065)

(4. 四川大学 原子核科学技术研究所 辐射物理及技术教育部重点实验室, 四川 成都 610065)

**摘要:** 研究了双重退火过程中保温时间对 Ti55511 钛合金显微组织和拉伸性能的影响。结果表明, 初生  $\alpha$  ( $\alpha_p$ ) 相的形态和尺寸主要受第一阶段保温时间的影响。随着保温时间的增加, 在末端迁移机制的驱使下, 长条状的  $\alpha_p$  转变为短棒状而发生宽化生长, 而当保温时间超过 2 h,  $\alpha_p$  生长变缓。 $\alpha_p$  的体积分数主要受第二阶段保温时间的影响, 随着保温时间的增加,  $\alpha_p$  的体积分数增加, 同时也影响了次生  $\alpha$  ( $\alpha_s$ ) 相的析出。Ti55511 合金的力学性能受  $\alpha_p$  和  $\alpha_s$  共同影响。拉伸试验结果表明, 双重退火过程中最佳保温时间范围为第一阶段的有效保温时间 1~4 h, 第二阶段有效保温时间 0.5~2 h。

**关键词:** Ti55511 钛合金; 热处理; 保温时间; 显微组织; 拉伸性能

作者简介: 罗恒军, 男, 1982 年生, 博士生, 正高级工程师, 湖南大学材料科学与工程学院, 湖南 长沙 410082, E-mail: luohengjun2022@163.com